Available online at www.sciencedirect.com
SCIENCE DIRECT®
European Journal of Pharmaceutical Sciences 21 (2004) 635–644
EUROPEAN JOURNAL OF PHARMACEUTICAL SCIENCES
www.elsevier.com/locate/ejps

Block of human $Na_V1.5$ sodium channels by novel α-hydroxyphenylamide analogues of phenytoin

Paul W. Lenkowski [a], Seong-Hoon Ko [b], James D. Anderson [a], Milton L. Brown [a], Manoj K. Patel [b,*]

[a] *Department of Chemistry, University of Virginia, McCormick Road, Box 400319, Charlottesville, VA 22904, USA*
[b] *Department of Anesthesiology, University of Virginia Health System, Box 800710, Charlottesville, VA 22908-0710, USA*

Received 22 October 2003; received in revised form 2 January 2004; accepted 8 January 2004

Abstract

Voltage-gated sodium (Na) channels are a critical component of electrically excitable cells. Phenytoin (diphenylhydantoin, DPH) is an established sodium channel blocker and is a useful anticonvulsant and class 1b antiarrhythmic, and has been effectively used in the treatment of neuropathic pain. In this study, we have synthesized novel α-hydroxyphenylamide analogues of diphenylhydantoin and examined their ability to inhibit human $Na_v1.5$ sodium channels expressed in Chinese Hamster Ovary (CHO-K1) cells. Phenyl ring substitutions were examined including *para*-methyl, *para*-fluoro, *para*-chloro, *ortho*-chloro and *meta*-chloro. We have found that phenyl ring substitutions with electron withdrawing properties resulted in compounds with greater activity. In comparison to diphenylhydantoin, the novel chloro-substituted α-hydroxyphenylamide compounds produced as much as a 20-fold greater tonic and frequency-dependent blockade of $Na_v1.5$ channels with an IC_{50} value of 14.5 μM. In addition, the chloro-substitutions have position specific state dependent blocking properties. The *ortho*-, *meta*- and *para*-chloro substitutions have an 8-, 13- and 3-fold increased affinity for the inactivated state, respectively. Molecular modeling suggests that these differences in affinity are due to a direct interaction with the receptor. Comparing models of diphenylhydantoin to the novel α-hydroxyphenlyamide compound suggests that the increased activity may be due to an optimized phenyl ring position and increased molecular volume. This information may be useful in the development of more potent sodium channel blockers.

Keywords: Sodium channels; α-Hydroxyphenylamide; Phenytoin

1. Introduction

Voltage-gated sodium (Na) channels play an important role in the generation and conduction of both cardiac and neuronal action potentials. They are composed of a pore forming α subunit and auxiliary β subunits that modulate gating properties of the channel (Catterall, 2000). To date nine α isoforms have been cloned (Goldin, 2001) and four β subunits, β1 (Isom et al., 1992), β2 (Isom et al., 1995), β3 (Morgan et al., 2000) and β4 (Yu et al., 2003).

Sodium channel blockers have proven extremely useful targets for the treatment of many diseases. For example Diphenylhydantoin (DPH) or Phenytoin is a clinically useful anticonvulsant, class 1b antiarrhythmic and has been effectively used in the treatment of neuropathic pain by virtue of its ability to block voltage-gated sodium channels (Barber et al., 1991; Willow et al., 1985; Tunnicliff, 1996; McCleane, 1999; Backonja, 2002). Sodium channel blockers such as local anesthetics and antiarrythmics mediate their block of sodium channels by two mechanisms, tonic (resting) block and use-dependent block (Hille, 1977; Hondeghem and Katzung, 1977). Tonic block results from low affinity binding of drug to the resting state of the channel whilst during use-dependent block drugs binds to the inactivated state of the channel with a greater affinity resulting in further inhibition of the current (Bean et al., 1983). Since sodium channel isoforms differ in channel gating kinetics these differences are thought to explain different affinities of sodium channel blockers for the various isoforms. For example, liodocaine has been shown to have a higher affinity for the $Na_v1.5$ isoform in comparison to the skeletal muscle specific isoform $Na_v1.4$ and neuronal sodium channel alpha

* Corresponding author. Tel.: +1-434-924-9586; fax: +1-434-924-2105.
E-mail address: mkp5u@virginia.edu (M.K. Patel).

0928-0987/$ – see front matter © 2004 Elsevier B.V. All rights reserved.
doi:10.1016/j.ejps.2004.01.004

subunits (Makielski et al., 1999; Pugsley and Goldin, 1998; Nuss et al., 2000; Bean et al., 1983).

Many sodium channel blocking analogues have been synthesized in order to develop more potent and selective sodium channel blockers. Therefore, we have synthesized novel α-hydroxyphenylamide compounds designed using the pharmacophore model developed for DPH (Brown et al., 1999) and examined their ability to inhibit the human sodium channel denoted $Na_v1.5$. Our data suggest that in comparison to DPH, the novel α-hydroxyphenylamide analogues examined herein induce profoundly greater tonic and frequency-dependent blockade of $Na_v1.5$ channels. In addition, we have found that the position of chloro substitutions on the phenyl ring in α-hydoxyphenylamides profoundly affects state dependent blocking properties. We demonstrate that DPH can be modified to have much greater blocking potency on $Na_v1.5$ sodium channels, providing useful data for the design of novel antiarrhythmic, anticonvulsant and analgesic agents.

2. Materials and methods

2.1. Chemistry

Compound 1 was synthesized as previously described by Brown et al. (1999). All compounds were prepared as represented in Scheme 1. Ketones were prepared in the following manner. To a flame-dried, round bottomed flask equipped with a magnetic stir bar and fitted with an inlet for maintaining an inert N_2 atmosphere, crushed magnesium (1.2 eq.) and one crystal I_2 were added. The flask was heated gently until I_2 vapor was produced. The flask was cooled to RT and heptyl bromide (1.1 eq.) in 10 ml ether was added dropwise. The reaction was stirred for 30 min then the nitrile (1 eq.) in 20 ml ether and CuBr were added. The reaction was refluxed gently under N_2 for 30 min and cooled to room temperature. Five milliliters water followed by 30 ml 15% H_2SO_4 were cautiously added and the heterogeneous mixture was stirred at RT for 24 h. The mixture was then extracted with EtOAc (3×25 ml) and the organic extracts were dried ($MgSO_4$) and the solvent removed in vacuo. The crude ketones were purified by flash column chromatography (10% EtOAc/90% hexanes) to give pure substituted ketones.

Cyanohydrins were prepared from ketones in the following manner. To a flame-dried, three-neck, round bottomed flask containing a magnetic stir bar and fitted with an inlet for maintaining an inert N_2 atmosphere, the ketone (1.0 eq.) dissolved in dry CH_2Cl_2 was added. Trimethylsilyl cyanide (2.2 eq.), KCN and 18-crown-6 (10 mg for every 1.0 mmol of ketone) were added and the reaction was monitored by loss of the carbonyl peak (2250 cm^{-1}) in the IR. The CH_2Cl_2 was evaporated in vacuo, and a minimal amount of dry THF was added. The mixture was cooled to 0 °C and 15% HCl (5 ml) was added and then stirred at room temperature for 2 h. The solution was combined with H_2O and extracted with Et_2O (3×25 ml), dried over $MgSO_4$, filtered, and concentrated to yield a thick dark oil. Because of stability concerns, the crude cyanohydrin was used without purification.

α-Hydroxyamides were prepared from cyanohydrins in the following manner. The cyanohydrin was dissolved in 1,4-dioxane (2 ml) and added to a round-bottomed flask while stirring. The mixture was cooled to 0 °C, and previously cooled (0 °C) concentrated HCl (0.2 ml for every 1 mmol of cyanohydrin) was added. HCl gas was then passed through the reaction mixture for 45 min at 0 °C. The mixture was allowed to stir at room temperature overnight. The mixture was extracted with EtOAc (3×25 ml), dried over $MgSO_4$, filtered and concentrated to yield the crude α-hydroxyphenylamides. Purification was performed by FCC (1:1 hexanes:EtOAc), collecting all fractions with a component of $R_f = 0.28$ to yield the pure α-hydroxyphenylamides.

Compound 1: 2-Hydroxy-2-phenyl-nonanoic acid amide. ^{1}H NMR: δ 0.86 (t, 3H), 1.07–1.47 (m, 10H), 2.01 (m, 1H), 2.2 (m, 1H), 3.52 (broad, 1H), 5.88 (s, 1H), 6.46 (s, 1H), 7.2–7.66 (m, 5H).

Compound 2: 2-(4-Methyl-phenyl)-2-hydroxy-nonanoic acid amide. ^{1}H NMR: δ 0.85 (t, 3H), 1.29 (m, 10H), 1.99 (m,1H), 2.19 (m, 1H), 2.35 (s, 3H), 3.06 (broad, 1H), 5.75 (s, 1H), 6.39 (s, 1H), 7.18–7.47 (m, 4H).

Compound 3: 2-(4-Fluoro-phenyl)-2-hydroxy-nonanoic acid amide. ^{1}H NMR: δ 0.85 (t, 3H), 1.28 (m, 10H), 2.01

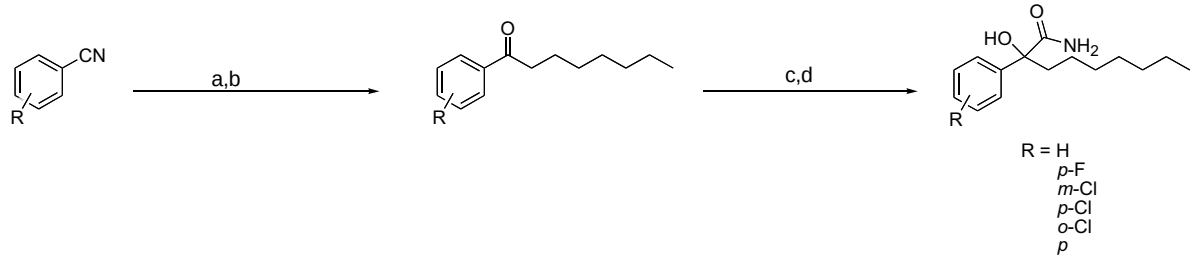

Scheme 1. Synthesis of the series of α-hydroxyphenylamides from substituted phenyl nitriles as described in detail in Section 2. The reagents used in each step are as follows: (a) heptyl magnesium bromide, ether, CuBr, reflux, 30 min; (b) 15% H_2SO_4, RT 24 h; (c) TMSCN, KCN, 18-crown-6, RT 3 h; (d) dioxane, HCl, HCl gas, 0 °C, 3 h.

(m,1H), 2.22 (m, 1H), 3.09 (broad, 1H), 5.59 (s, 1H), 6.45 (s, 1H), 6.95–7.62 (m, 4H).

Compound 4: 2-(4-Chloro-phenyl)-2-hydroxy-nonanoic acid amide. ^{1}H NMR: δ 0.86 (t, 3H), 1.25–1.30 (m, 10H), 1.99 (m,1H), 2.18 (m, 1H), 3.14 (broad, 1H), 5.64 (s, 1H), 6.46 (s, 1H), 7.30–7.54 (m, 4H).

Compound 5: 2-(2-Chloro-phenyl)-2-hydroxy-nonanoic acid amide. ^{1}H NMR: δ 0.85 (t, 3H), 1.31 (m, 10H), 1.99 (m,1H), 2.25 (m, 1H), 3.2 (broad, 1H), 5.84 (s, 1H), 6.55 (s, 1H), 7.23–7.61 (m, 4H).

Compound 6: 2-(3-Chloro-phenyl)-2-Hydroxy-nonanoic acid amide. ^{1}H NMR: δ 0.87 (t, 3H), 1.27 (m, 10H), 1.98 (m,1H), 2.19 (m, 1H), 3.23 (broad, 1H), 5.96 (s, 1H), 6.55 (s, 1H), 7.24–7.59 (m, 4H). Log P was calculated using the log P method described by Leo (1993).

2.2. Cell culture

Chinese Hamster Ovary (CHO-K1) cells stably expressing Nav1.5 were grown in DMEM/F12 media (Invitrogen Corp., CA, USA) supplemented with 10% fetal bovine serum, penicillin (100 U/ml), streptomycin (100 μg/ml) and G418 (500 μg/ml; Sigma, MO, USA). Cells were grown in a humidified atmosphere of 5% CO_2 and 95% air at 37 °C.

2.3. Electrophysiology

Sodium currents were recorded using the whole-cell configuration of the patch clamp recording technique with an Axopatch 200B amplifier (Axon Instruments, Foster City, CA). All voltage protocols were applied using pCLAMP 8 software (Axon, USA) and a Digidata 1322A (Axon, USA). Currents were amplified and low pass filtered (2 kHz) and sampled at 33 kHz. Borosilicate glass pipettes were pulled using a Brown-Flaming puller (model P87, Sutter Instruments Co., Novato, CA) and heat polished to produce electrode resistances of 0.5–1.5 MΩ when filled with the following electrode solution (in mM); CsCl 130, $MgCl_2$ 1, MgATP 5, BAPTA 10, HEPES 5 (pH adjusted to 7.4 with CsOH). Cells were plated on glass coverslips and superfused with solution containing the following composition (in mM) NaCl 130, KCl 4, $CaCl_2$ 1, $MgCl_2$ 5, HEPES 5, and glucose 5 (pH adjusted to 7.4 with NaOH). Compounds were prepared as 100 mM stock solutions in dimethly sulfoxide (DMSO) and diluted to desired concentration in perfusion solution. The maximum DMSO concentration used was 0.3% and had no effect on current amplitude. All experiments were performed at room temperature (20–22 °C). After establishing whole-cell, a minimum series resistance compensation of 75% was applied and cells were held at −80 mV for 5 min to account for equilibrium gating shifts. Voltage error was calculated using the following equation:

$$\Delta V = I_p(1 - a)R$$

where ΔV is the voltage error, I_p the peak current, a the series resistance compensation and R the series resistance. Data from cells with a voltage error greater than 3 mV were excluded. Activation and steady-state inactivation data were fitted by the equation:

$$y = \frac{1}{1 + \exp((V - V_{1/2})/k)}$$

where y is the normalized conductance (g/g_{max}) or the normalized current for activation and inactivation, respectively, $V_{1/2}$ the voltage of half-maximal activation or inactivation and k the slope factor. The difference between the $V_{1/2}$ value in the presence and absence of compound is shown as $\Delta V_{1/2}$ (mV). Time constants for recovery from inactivation were obtained using a double exponential function:

$$y = A_1\left(1 - \exp\left(-\frac{t}{\tau_1}\right)\right) + A_2\left(1 - \exp\left(-\frac{t}{\tau_2}\right)\right)$$

A_1 and A_2 are the coefficients for the fast and slow exponentials, t the time (ms) and τ_1 and τ_2 the fast and slow time constants. The percentage of the current represented by the fast time constant was calculated from the equation $100\% \times A_1/(A_1+A_2)$, where A_1 and A_2 are the amplitudes of the fast and slow gating modes, respectively. Time constants for use-dependent block were obtained using the equation:

$$y = A\exp\left(-\frac{t}{\tau}\right) + C$$

where A is the coefficient of the exponential, t the time (ms), τ the time constant (ms) and C the fraction of unblocked current at the end of the time course.

2.4. Data analysis

All data analysis was performed using Clampfit software (v8, Axon Instruments, CA, USA), Origin (v5, Microcal Software, MA, USA), and Excel (Microsoft). Statistical analyses were performed using a t-test for normally distributed data as determined by the Kolmogorov–Smirnov test, or the Rank Sum test for non-normalized data (Sigma Stat, Jandel). Averaged data are presented as means ± standard error of the mean (S.E.M.). Values of $P < 0.05$ were considered to indicate significance.

2.5. Molecular modeling

The X-ray coordinates for phenytoin (DPH) were utilized in this study (Camerman and Camerman, 1971). The α-hydroxyphenylamides were modified from the X-ray structure and were energy-minimized with the Tripos force field using conjugate gradient approach and 0.05 kCal/mol energy cutoff, without solvent, using default bond distances and angles and neglecting electrostatics. The minimization was completed by aggregating using the SYBYL/AGGREGATE module for only the X-ray structure atoms and allowing the modified portion to minimize. For internal consistency, we used only the R-configuration for all chiral compounds. For compounds 1–6, the plane angles

were calculated using the phenyl ring for plane 1 and the carbonyl and nitrogen of the amide for plane 2. Plane 1 for DPH was constructed with phenyl ring atoms and plane 2 using all hydantoin ring atoms. The plane angle was calculated as the angle between planes 1 and 2. Molecular volume was determined using the volume contour option within SYBYL/VIEW presented with default options.

3. Results

3.1. Tonic block by novel α-hydroxyphenylamide analogue

In this study, we have examined α-hydroxyphenylamide analogues of DPH (compounds 1–6) and focused on the relationship between blockade of sodium current with substitutions on the phenyl ring. Fig. 1 summarizes the compounds examined in this study. Tonic block was assessed by a step depolarization to +20 mV for 25 ms from a holding potential of −120 mV. We initially assessed the *para* position of the phenyl ring and examined methyl (compound 2), fluoro (compound 3) and chloro (compound 4) substitutions. These were compared to the unsubstituted phenyl ring (compound 1) and DPH. Fig. 2A shows the dose response relationship for these analogues. Representative currents traces for tonic block by DPH are shown as the upper inset in Fig. 2A but data were excluded from the dose response figure for clarity. It is clear from Fig. 2A that the most efficient block occurred with a chloro substitution on the phenyl ring (compound 4). Representative current traces for the tonic block by compound 4 are shown in the lower inset of Fig. 2A. The order of potency determined was chloro > fluoro > unsubstituted > methyl ∼ DPH (Table 1). We were unable to determine IC_{50} values for DPH and compound 2 as their maximum solubility's were less than 200 μM. The highest concentration tested for DPH and compound 2 was 100 μM inducing 23.4 ± 6.0% ($n = 4$) and 28.6 ± 7.2% ($n = 5$) block, respectively.

The position of phenyl ring substitutions can have a profound impact on ligand–receptor interactions (Brown et al., 1997; Deutsch et al., 1996). In view of this, we sought to determine the optimal phenyl ring substitution position for our most potent inhibitor (compound 4). Compounds 5 and 6 were synthesized and represent the *ortho*- and *meta*-chloro substitutions, respectively. Fig. 2B shows the dose response relationship for the *ortho*-, *meta*- and *para*-chloro-substituted α-hydroxyphenylamides. Representative currents traces for tonic block by compounds 5 and 6 are shown in the inset of Fig. 2B. Although the *para*- and *meta*-chloro-substituted α-hydroxyphenylamide compounds have similar IC_{50} values, their Hill coefficients were significantly different and could suggest different types of interactions. However, both of these positions were nearly six-fold more potent then the *ortho*-chloro substitution. Furthermore, compounds 5 and 6 had similar Hill coefficients and thus may be interacting with the channel in a similar

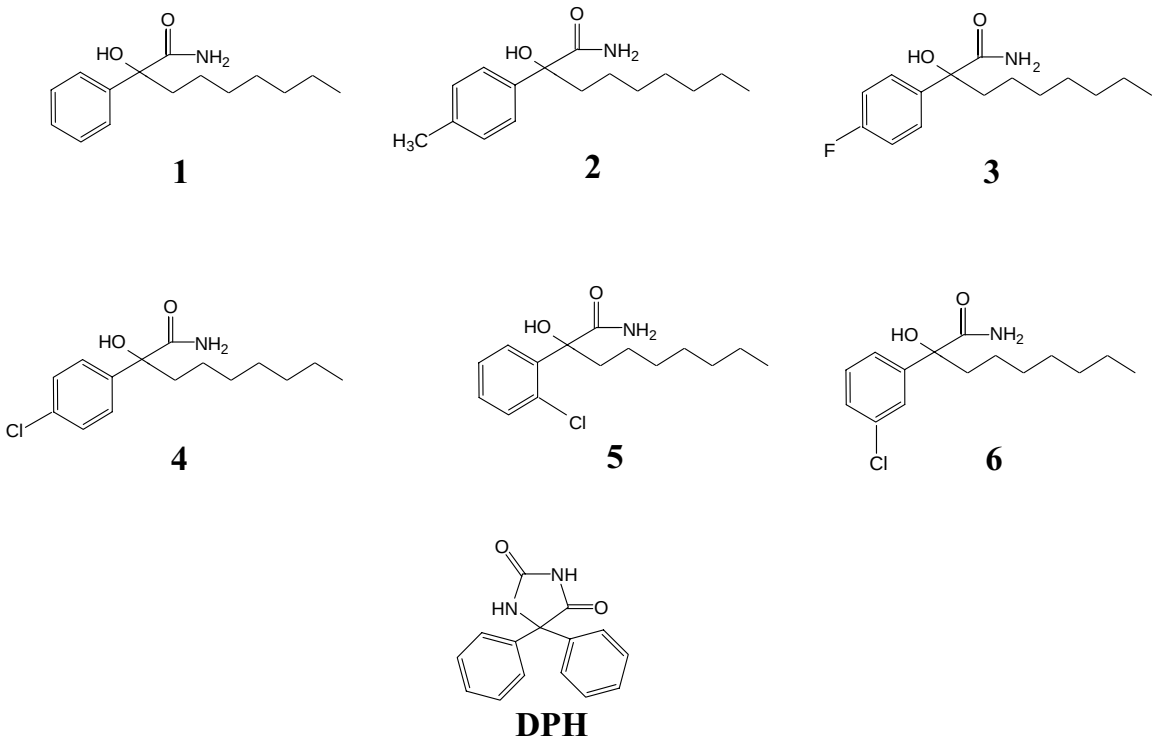

Fig. 1. Compound structures. DPH and novel α-hydroxyphenylamide substitutions examined in this study. Structures show differences in phenyl ring substitution. Compounds 1 is unsubstituted. Compounds 2, 3 and 4 are the *para*-methyl, *para*-fluoro and *para*-chloro substitutions, respectively. Compounds 5 and 6 are the *ortho*- and *meta*-chloro substitutions, respectively.

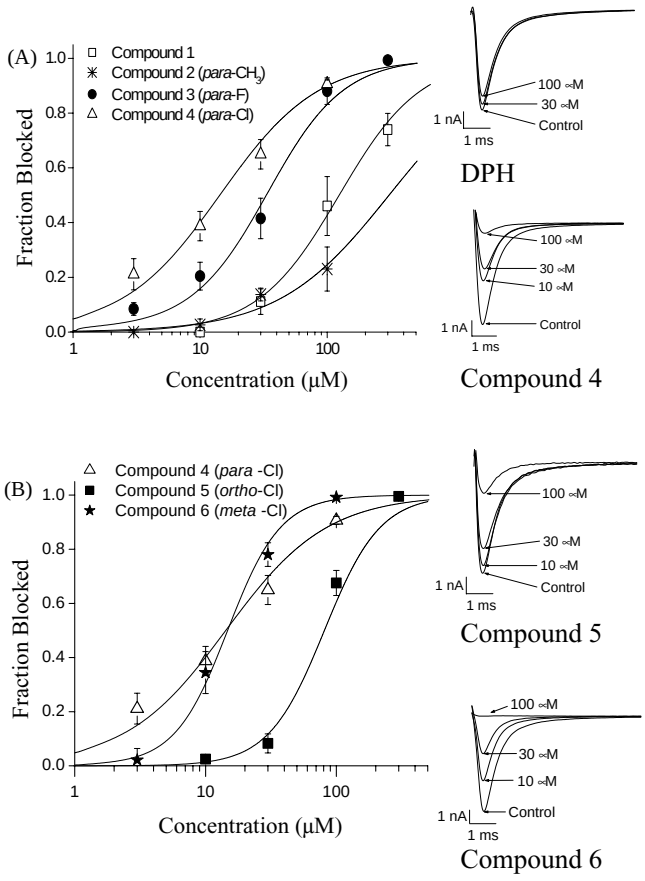

Fig. 2. Tonic block by novel α-hydroxyphenylamides. Currents were elicited by a step depolarization to +20 mV for 25 ms from a holding potential of −120 mV. (A) Dose response relationship for the *para*-substituted α-hydroxyphenylamide analogues. Inset shows representative current traces for the application of DPH and compound 4. (B) Dose response relationship for *ortho*-, *meta*- and *para*-chloro-substituted α-hydroxyphenylamide analogues. Inset shows representative current traces for the application of compounds 5 and 6. Data represent mean ± S.E.M. Smooth lines represent the least squares fit when data were fitted with the Hill equation.

manner despite their different affinities for the channel. Table 1 summarizes the IC_{50} values and Hill coefficients for compounds 1 and 3–6.

3.2. Current–voltage relationship and channel activation

We examined the effects of the novel α-hydroxyphenylamides and DPH on channel activation. The current–voltage relationship was determined with a 20 ms voltage step ranging from −80 to +60 mV in steps of 5 mV from a holding potential of −120 mV at 2 s intervals. The peak of the current–voltage relationship was +5 mV for control and was unchanged in presence of any compound examined (data not shown). In order to assess for effects on channel activation, the voltage dependence of channel conductance was derived from the current–voltage relationship as described in Section 2. The half activation and slope values for control data were −15.8 ± 1.7 and −7.7 ± 0.2 mV, respectively and

Table 1
IC_{50} and Hill coefficient (n_H) parameters for tonic block of $Na_v1.5$ by novel α-hydroxyphenylamide compounds

Compound	IC_{50} (μM)	n_H	n	Log P
DPH	N.D.	N.D.	4	2.09
1	132.9 ± 31.0	1.2 ± 0.3	5	3.43
2	N.D.	N.D.	5	3.93
3	32.2 ± 7.4	1.5 ± 0.1	4	3.57
4	14.3 ± 2.7	1.1 ± 0.2	7	4.14
5	81.8 ± 7.0	2.1 ± 0.1	7	4.14
6	14.7 ± 1.8	2.1 ± 0.4	6	4.14

IC_{50} and Hill coefficients were calculated using the Hill equation. Values represent the mean ± S.E.M.; N.D. (not determined).

were not significantly changed in the presence of any of the compounds examined (data not shown).

3.3. Steady-state inactivation

To further investigate the mechanism of block, we examined the effects of the novel α-hydroxyphenylamide compounds on steady-state inactivation. Compounds that have a higher affinity for the inactivated state of the channel shift the steady inactivation curve in a hyperpolarized direction. All compounds were examined at 30 μM with exception of DPH, which was examined at 100 μM. In addition, compound 5 was examined at 100 μM for comparison to compounds 4 and 6 in order to account for differences in the IC_{50} values. Fig. 3 demonstrates the effects of compounds 4 (30 μM), 5 (100 μM) and 6 (30 μM) on steady-state inactivation. The shift of the midpoint of

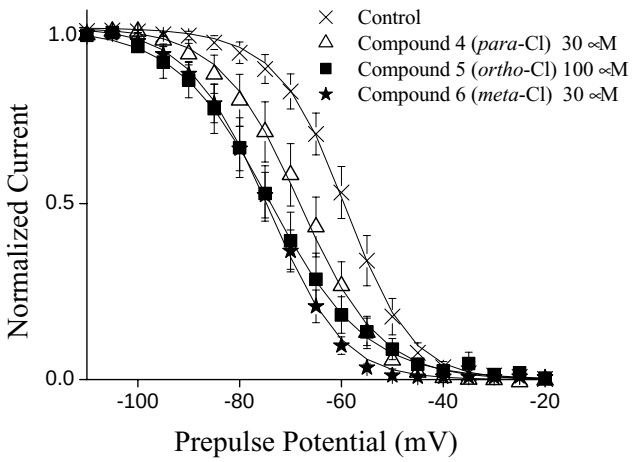

Fig. 3. Chlorinated α-hydroxyphenylamide compounds alter the steady-state inactivation properties of the $Na_v1.5$ channel. From a potential of −120 mV, prepulse potentials ranging from −120 to −20 mV were applied for 1 s followed by a depolarizing step to +20 mV to elicit sodium current. Currents were normalized to the peak current elicited from the −120 mV holding potential within each experiment. Data points represent the mean ± S.E.M. Smooth lines correspond to the average of the least squares fits when data were fitted by the Boltzmann equation as described in Section 2. Compounds 4 and 6 were examined at 30 μM and compound 5 was examined at 100 μM. The half inactivation and slope values for control data were −60.0 ± 2.0 and 6.0 ± 0.3 mV, respectively.

Table 2
The effects of novel α-hydroxyphenylamide compounds on $Na_v1.5$ channel steady-state inactivation parameters

Compound	k (mV)	$\Delta V_{1/2}$ (mV)
DPH (100 μM)	6.9 ± 0.6	3.6 ± 1.1
Compound 1	7.0 ± 0.7	6.1 ± 0.6
Compound 3	6.8 ± 0.7	6.5 ± 0.5
Compound 4	6.1 ± 0.3	4.6 ± 0.9
Compound 5	7.0 ± 1.0	5.5 ± 0.6
Compound 5 (100 μM)	7.6 ± 0.4	11.9 ± 1.0[a,***]
Compound 6	6.6 ± 0.3	14.8 ± 0.9[a,***]

Steady-state inactivation data were fitted by the Boltzmann equation as described in Section 2. All compounds were examined at 30 μM unless otherwise noted. Values represent the mean ± S.E.M.

[a] Denotes a lack of significance between compounds 5 and 6 ($P = 0.409$).

*** $P < 0.001$.

the steady-state inactivation curve ($\Delta V_{1/2}$) and slope (k) values for all compounds are summarized in Table 2. The half inactivation ($V_{1/2}$) and k values for control data were -60.0 ± 2.0 and 6.0 ± 0.3 mV, respectively. DPH and all of the novel α-hydroxyphenylamides examined significantly shifted the midpoint of the steady-state inactivation curve (paired t-test). None of the compounds studied significantly affected the k values. Compound 6 (*meta*-chloro) at 30 μM and compound 5 (*ortho*-chloro) at 100 μM induced a significantly ($P < 0.001$) greater shift in the $V_{1/2}$ value compared to compound 4 (*para*-chloro; Fig. 3 and Table 2). These data suggest that compounds 5 and 6 have a higher affinity for the inactivated state of the channel than compound 4. From the steady-state inactivation shift and the dose response relationship, the apparent affinity for the inactivated state (K_i) was calculated using the equation:

$$K_i = \frac{D}{((1 + D/K_r)/e^{\Delta h/k}) - 1}$$

where Δh is the shift of the steady-state curve, k the slope of the steady-state inactivation curve, K_r the affinity for the resting state (IC_{50}) taken from the dose response curve and D the drug concentration responsible for the steady-state inactivation shift (Bean et al., 1983; Gomora et al., 2001). When the IC_{50} value is used as the K_r value, the K_i value represents the IC_{50} for the inactivated state. The calculated affinities for the inactivated states for compounds 4, 5 and 6 were 5.3, 10.2 and 1.1 μM, respectively. Examining the ratio of the affinity for the resting state to the affinity for the inactivated state allows for direct comparison of compounds with different IC_{50} values. The calculated ratios (K_r/K_i) were 3, 8 and 13 and for compounds 4, 5 and 6, respectively. While compound 5 had the lowest affinity for the inactivated state (K_i), an examination of the ratio of K_r/K_i demonstrated that compounds 5 and 6 had a much increased selectivity for the inactivated state when compared to compound 4. In order to further examine this differential affinity for the inactivated states, we examined channel recovery from inactivation at −90 mV.

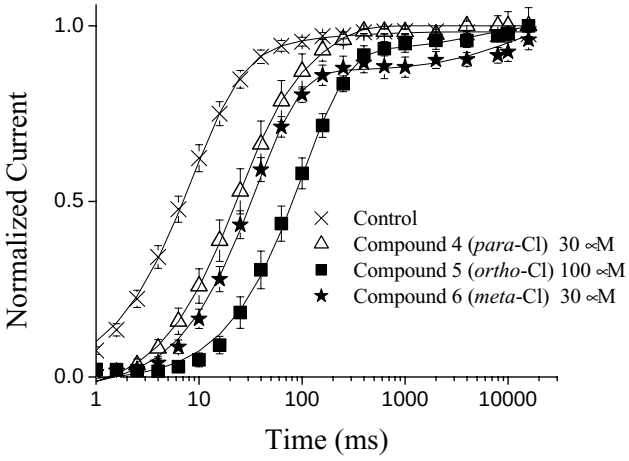

Fig. 4. Novel α-hydroxyphenylamide compounds slow recovery from inactivation. Compounds 4 and 6 were examined at 30 μM and compound 5 was examined at 100 μM. Recovery from inactivation was assessed using a two-pulse protocol. A pre-pulse from −120 to +20 mV for 100 ms was applied to inactivate all channels. Cells were then held at −90 mV for a variable period (1–15,800 ms) to allow channels to recovery and then the proportion of recovered channels was assessed with a voltage step to +20 mV. Current amplitude is normalized to the peak current recorded in the protocol. Data are plotted on a logarithmic time scale. Data points represent the mean ± S.E.M. Smooth lines correspond to the average of the least squares fits when data were fitted by a double exponential function as described in Section 2.

3.4. Recovery from inactivation

Compounds that have higher affinity for the inactivated state of the channel may delay recovery from inactivation. Thus, we sought to determine how the novel α-hydroxyphenlyamide compounds affect recovery from inactivation at −90 mV. Recovery from inactivation was assessed using a two-pulse protocol. A pre-pulse from −120 to +20 mV for 100 ms was applied to inactivate all channels. Cells were then held at −90 mV for a variable period (1–15,800 ms) to allow channels to recovery and then the proportion of recovered channels was assessed with a voltage step to +20 mV. Fig. 4 demonstrates the effects of compounds 4 and 6 at 30 μM and compound 5 at 100 μM on recovery from inactivation. Currents were normalized to the peak current at the last time point and data were plotted on a logarithmic time scale for clarity. Recovery data were fitted by a double exponential function as described in Section 2 and the effects of DPH and the novel α-hydroxyphenylamide compounds on fit parameters are summarized in Table 3.

Compounds 1–6, but not DPH significantly delayed channel recovery. However, only compounds 4–6 significantly affected the second time constant of recovery. It is interesting to note that the second time constant (τ_2) for compounds 5 and 6 were significantly different from compound 4 but not from each other suggestive that compounds 5 and 6 affected the channel distinctively. The recovery data suggests that channels blocked by 30 μm of compound 4 reach steady state near 200 ms whereas only a proportion of channels are recovered in presence of compound 5 or 6. Thus, we ex-

Table 3
The effects of novel α-hydroxyphenylamide compounds on the recovery from inactivation

Condition	τ_1 (ms)	τ_2 (ms)	Fast (%)
Drug Free	6.8 ± 1.1	43.7 ± 5.3	76.5 ± 4.0
DPH (100 μM)	18.0 ± 8.8	57.1 ± 10.9	67.1 ± 12.6
Compound 1	14.8 ± 1.5	67.7 ± 6.8	57.2 ± 2.2
Compound 3	13.8 ± 2.8	62.1 ± 9.1	68.4 ± 4.1
Compound 4	22.1 ± 2.2	97.3 ± 15.1	71.4 ± 0.1
Compound 5	35.1 ± 5.7	357.9 ± 110.1	56.1 ± 12.4
Compound 5	100.4 ± 17.6	2.3 ± 1.3 s[a,***]	88.3 ± 7.2
Compound 6	35.2 ± 4.2	5.6 ± 1.1 s[a,***]	84.1 ± 4.0

Recovery data were fitted by a double exponential function as described in Section 2. Values represent the mean ± S.E.M.

[a] Denotes a lack of significance between compounds 5 and 6 ($P = 0.409$).

*** $P < 0.001$.

amined the kinetics of use-dependent block at 5 Hz (200 ms interval).

3.5. Use-dependent block

Use-dependent block by DPH and the novel chlorinated α-hydroxyphenylamide analogues (compounds 4–6) was assessed at 5 Hz train frequency from a holding potential of −90 mV. Currents were normalized to the first pulse in each experiment and the results are plotted in Fig. 5A. Example current traces are shown in Fig. 5B. These results suggest differences in the rate of onset and extent of use-dependent block. Compounds 4–6 produced significantly greater use-dependent block than DPH ($P < 0.001$). Compound 6 (30 μM) produced significantly greater use-dependent block compared to compounds 4 (30 μM) and 5 (100 μM), block-

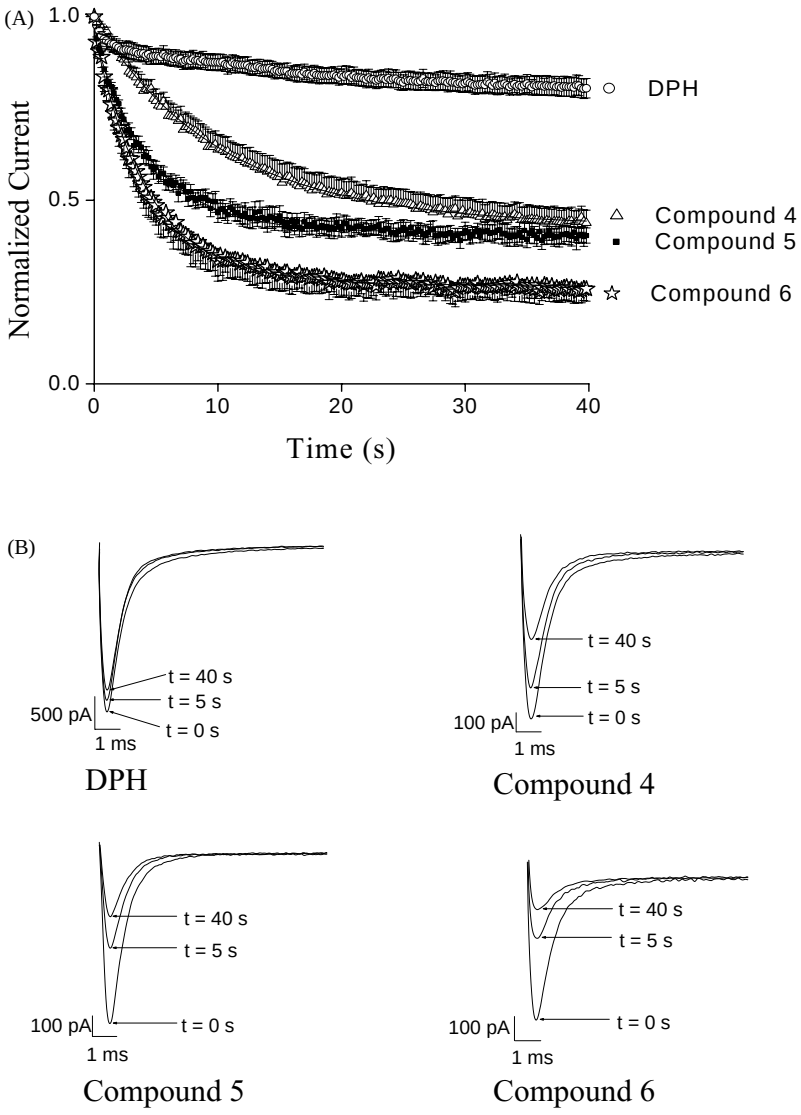

Fig. 5. (A) Use-dependent block by DPH and novel chlorinated α-hydroxyphenylamides. DPH and compound 5 were examined at 100 μM and compounds 4 and 6 were examined at 30 μM. Cells were held at −90 mV and a voltage step to 20 mV was applied for 25 ms at a frequency of 5 Hz. Smooth lines correspond to the average of the least squares fits when data were fitted by a single exponential function as described in Section 2. (B) Representative current traces showing the first pulse, a pulse 5 s into the protocol and the last pulse.

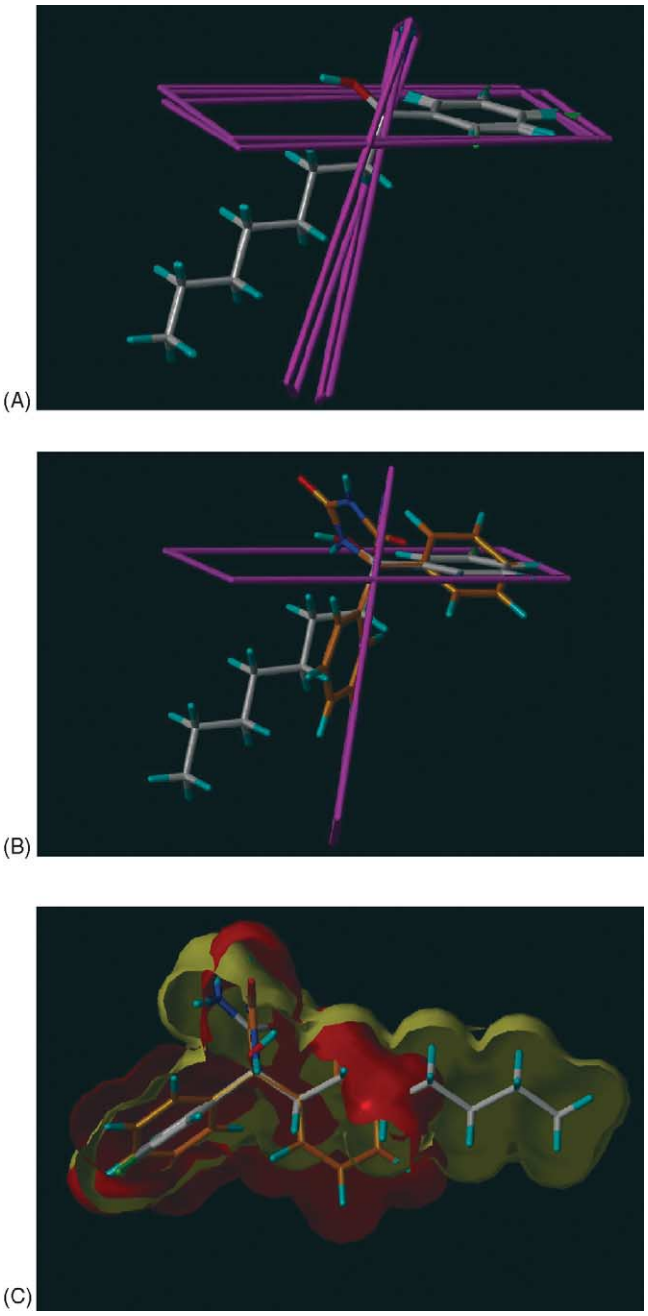

Fig. 6. Molecular modeling. The X-ray coordinates for phenytoin (DPH) were utilized in this study. The α-hydroxyphenylamides were modified from the X-ray structure and were energy-minimized with the Tripos force field using conjugate gradient using default bond distances and angles and neglecting electrostatics. The minimization was completed by aggregating using the SYBYL/AGGREGATE module for only the X-ray structure atoms and allowing the modified portion to minimize. For internal consistency, we used only the *R*-configuration for all chiral compounds. (A) Overlap of 3D structures of compounds 4–6. The plane containing the phenyl ring and a plane containing the amide are outlined in purple to demonstrate the effects of chloro position on 3D structure. (B) Overlap of compound 6 and DPH demonstrating the different relative position of the phenyl rings. (C) Molecular volume was determined using the volume contour option within SYBYL/VIEW presented with default options. DPH is shown in red and compound 6 in yellow.

ing 74.1 ± 3.3% of the current at steady state ($P < 0.05$). DPH, compounds 4 and 5 blocked 19.5 ± 2.6, 56.2 ± 3.5 and 59.6 ± 2.1% of sodium currents, respectively, at steady state. There were no significant differences in the extent of use-dependent block between compounds 4 and 6. To assess the rate of development of use-dependent block, data were fitted by a single exponential function as described in Section 2. Time constants for onset of use-dependent block were 9.5 ± 1.5 and 10.7 ± 1.0 s for DPH and compound 4, respectively, and were not significantly different. The time constants for compounds 5 and 6 were 4.6 ± 0.3 and 4.0 ± 0.4 s, respectively, and were not significantly different from each other, but were significantly different from compound 4 and DPH ($P < 0.001$). This further confirms that compounds 5 and 6 are acting in a distinct manner compared to compound 4.

3.6. Molecular modeling

Compound 5 (*ortho*-chloro) had much lower affinity for the closed state of the channel in comparison to compounds 4 (*para*-chloro) and 6 (*meta*-chloro). This difference could be explained by changes in the 3D structure of compound 5 by repulsion of the phenyl ring away from the amide carbonyl due to steric interactions from the close approximation of the *ortho*-substituted chloride atom. In order to examine any potential differences in the three dimensional structures of compounds 4–6, molecular models were computed and compared as described in Section 2. The structures of compounds 4–6 were overlapped and are presented in Fig. 6A and planes containing the phenyl ring and amide group are delimited by purple lines. Examination of the angle formed between the plane of the phenyl ring and the plane of the amide revealed that the *para*-, *ortho*- and *meta*-chloro α-hydroxyphenylamides had similar angles (94.14°, 101.16° and 94.11° for compounds 4, 5 and 6, respectively; Fig. 6A). In order to examine potential molecular explanations for the increased affinity of compound 6, a low energy structure of compound 6 similar to the low energy conformer of DPH was compared to DPH (Fig. 6B). The phenyl ring of DPH is tilted ∼30° relative to the plane containing the phenyl ring of compound 6 suggesting a significantly different phenyl ring conformation. In order to examine the impact of these differences, overlaps of the molecular volumes of DPH (red) and compound 6 (yellow) were created and are demonstrated in Fig. 6C. Molecular volumes for compound 6 and DPH were calculated to be 253.1 and 199.5 Å^3, respectively. This data suggests that the binding sites within $Na_v1.5$ can tolerate larger molecules resulting in increased activity.

4. Discussion

4.1. Comparison with previous work

The development of α-hydroxyphenylamides as sodium channel blockers was based on a comparative molecular

field analysis (CoMFA) study of various hydantoins binding to neuronal sodium channels (Brown et al., 1999). CoMFA samples the differences in steric and electrostatic fields surrounding a set of ligands to help define important three-dimensional properties associated with the optimum binding of ligand to receptor. Employing the use of CoMFA, we have previously predicted and demonstrated that an unsubstituted α-hydroxyphenylamide (compound 1) possessed a four-fold lower IC_{50} value compared to DPH when examined using [^{3}H] batrachotoxinin A 20-α-benzoate (BTX) displacement from rat brain cerebral cortex synaptasomes (Brown et al., 1999). An important limitation to the previous study was the lack of functional data on the ability of these compounds to inhibit sodium currents. In this study, we examined the effects of novel DPH analogues on the human $Na_v1.5$ sodium channel clone expressed in a mammalian cell line. These results are relatively comparable to experiments with DPH in isolated ventricular myocytes as demonstrated by Grant and coworkers (Barber et al., 1991). Furthermore, the use of mammalian expression systems is generally accepted to accurately reflect the channel kinetics observed in primary cells (Chen et al., 2000).

Sodium channel gating can be described by three states; closed, opened and inactivated. The state of the channel studied using BTX displacement is unknown. However, it has been well established that DPH has a much higher affinity for the inactivated state of the channel and this information cannot be acquired using displacement studies (Kuo and Bean, 1994). Nevertheless, consistent with BTX displacement results, compound 1 blocked $Na_v1.5$ sodium channels with nearly three-fold greater affinity compared to DPH. This suggests that BTX displacement data correlates with data for functional block of sodium currents.

4.2. Mechanism of $Na_v1.5$ block

The dose response data suggests that the electron withdrawing substitutions of fluoro (compound 3) and chloro (compound 4) inhibit $Na_v1.5$ sodium channels more effectively than a non-substituted (compound 1) or electron donating methyl substitution (compound 2). In addition compound 4 (*para*-chloro) had a greater blocking activity than compound 3 (*para*-Fluoro). In agreement with previous results, a general trend of decreasing IC_{50} with increasing Log *P* was observed (Table 1) (Brown et al., 1997). This increased block seen by compound 4 may be due to increased stabilization of the π–π stacking interactions between the phenyl ring of compound 4 and an aromatic residue within the receptor site. Indeed, several studies have implicated the role of the aromatic amino acids F1760 and Y1767 in the S6 of domain IV of the $Na_v1.5$ sodium channel as necessary for high affinity binding of local anesthetics and other compounds (Mujtaba et al., 2002; Nau et al., 2000a; Nau et al., 2000b). Moreover, the noticeable increase in potency by the introduction of a chloro atom at the *para* position of the aromatic ring may be attributed to additional electrostatic and van der Waals interactions of the larger halogen atom within the receptor site.

The most potent compound examined in this series, compound 6, was able to block $Na_v1.5$ sodium currents with 20-fold greater affinity compared to DPH. The fact that compound 5 had a much higher IC_{50} value compared to compounds 4 and 6 is most likely due to a direct steric interaction with the receptor. Modeling of compounds 4–6 demonstrates that the position of the chloro substitution does not significantly alter the 3D structure of the compounds (Fig. 6A). Molecular modeling suggests that this series of compounds may be more potent than DPH because of a more optimal phenyl ring conformation and increased bulk from the alkyl side chain (Fig. 6B and C). An interesting outcome of this study was the observation that the position of the chloro group on the phenyl ring is related to state dependent block. Several lines of evidence support the fact that the *ortho*- and *meta*-chloro-substituted compounds have much greater relative affinity for the inactivated state of the channel compared to the *para* position. The distinctions between the *ortho* and the *meta* chloro as compared to the *para* chloro compound includes: the Hill coefficient, the steady-state inactivation shift, the relative affinity for the inactivated state, the effects on the second phase of recovery from inactivation and the effects on use-dependent block. These results may be in part due to limited access to the receptor in the closed state of the channel for the *ortho* and *meta*-substituted compounds. Nonetheless, this study demonstrates for the first time that state dependent block is dependent upon substitution position and this information could be used in the development of compounds with state selective blocking properties. We have developed novel α-hydroxyphenylamide analogues of DPH with profoundly greater tonic and frequency-dependent blockade of $Na_v1.5$ channels. This data may be useful in the design of novel antiarrhythmic, anticonvulsant and analgesic agents.

Acknowledgements

We thank Dr. A.O. Grant (Duke University, USA) for providing the $Na_v1.5$ stably transfected CHO cells and Dr. Carl Lynch III for helpful comments. This work was supported by a grant from the American Heart Association (Virginia Affiliate; M.K.P. and S.-H.K.) and The Korean Science and Engineering Foundation (S.-H.K.). We also thank the Medical Scientist Training Program and the Cardiovascular Research Center, University of Virginia (P.W.L.). We would also like to thank the Jefferies Trust Fund (J.D.A.).

References

Backonja, M.M., 2002. Use of anticonvulsants for treatment of neuropathic pain. Neurology 59, S14–S17.

Barber, M.J., Starmer, C.F., Grant, A.O., 1991. Blockade of cardiac sodium channels by amitriptyline and diphenylhydantoin. Evidence for two use-dependent binding sites. Circ. Res. 69, 677–696.

Bean, B.P., Cohen, C.J., Tsien, R.W., 1983. Lidocaine block of cardiac sodium channels. J. Gen. Physiol. 81, 613–642.

Brown, M.L., Brown, G.B., Brouillette, W.J., 1997. Effects of log *P* and phenyl ring conformation on the binding of 5-phenylhydantoins to the voltage-dependent sodium channel. J. Med. Chem. 40, 602–607.

Brown, M.L., Zha, C.C., Van Dyke, C.C., Brown, G.B., Brouillette, W.J., 1999. Comparative molecular field analysis of hydantoin binding to the neuronal voltage-dependent sodium channel. J. Med. Chem. 42, 1537–1545.

Camerman, A., Camerman, N., 1971. Stereochemical basis of anticonvulsant drug action. I. Crystal and molecular structure of diphenylhydantoin, a noncentrosymmetric structure solved by centric symbolic addition. Acta Crystallographica, Section B: Structural Crystallography and Crystal Chemistry 27 (11), 2205–2211.

Catterall, W.A., 2000. From ionic currents to molecular mechanisms: the structure and function of voltage-gated sodium channels. Neuron 26, 13–25.

Chen, Y.H., Dale, T.J., Romanos, M.A., Whitaker, W.R., Xie, X.M., Clare, J.J., 2000. Cloning, distribution and functional analysis of the type III sodium channel from human brain. Eur. J. Neurosci. 12, 4281–4289.

Deutsch, H.M., Shi, Q., GruszeckaKowalik, E., Schweri, M.M., 1996. Synthesis and pharmacology of potential cocaine antagonists. 2. Structure-activity relationship studies of aromatic ring-substituted methylphenidate analogs. J. Med. Chem. 39, 1201–1209.

Goldin, A.L., 2001. Resurgence of sodium channel research. Annu. Rev. Physiol 63, 871–894.

Gomora, J.C., Daud, A.N., Weiergraber, M., Perez-Reyes, E., 2001. Block of cloned human, T-type calcium channels by succinimide antiepileptic drugs. Mol. Pharmacol. 60, 1121–1132.

Hille, B., 1977. Local anesthetics: hydrophilic and hydrophobic pathways for the drug-receptor reaction. J. Gen. Physiol. 69, 497–515.

Hondeghem, L.M., Katzung, B.G., 1977. Time-and voltage-dependent interactions of antiarrhythmic drugs with cardiac sodium channels. Biochim. Biophys. Acta 472, 373–398.

Isom, L.L., De Jongh, K.S., Patton, D.E., Reber, B.F., Offord, J., Charbonneau, H., Walsh, K., Goldin, A.L., Catterall, W.A., 1992. Primary structure and functional expression of the beta 1 subunit of the rat brain sodium channel. Science 256, 839–842.

Isom, L.L., Ragsdale, D.S., De Jongh, K.S., Westenbroek, R.E., Reber, B.F., Scheuer, T., Catterall, W.A., 1995. Structure and function of the beta 2 subunit of brain sodium channels, a transmembrane glycoprotein with a CAM motif. Cell 83, 433–442.

Kuo, C.C., Bean, B.P., 1994. Slow binding of phenytoin to inactivated sodium-channels in rat hippocampal-neurons. Mol. Pharmacol. 46, 716–725.

Leo, A.J., 1993. Calculating log P_{oct} from structures. Chem. Rev. 93, 1281–1306.

Makielski, J.C., Limberis, J., Fan, Z., Kyle, J.W., 1999. Intrinsic lidocaine affinity for Na channels expressed in Xenopus oocytes depends on alpha (hH1 vs. rSkM1) and beta 1 subunits. Cardiovasc. Res. 42, 503–509.

McCleane, G.J., 1999. Intravenous infusion of phenytoin relieves neuropathic pain: A randomized, double-blinded, placebo-controlled, crossover study. Anesthesia Analgesia 89, 985–988.

Morgan, K., Stevens, E.B., Shah, B., Cox, P.J., Dixon, A.K., Lee, K., Pinnock, R.D., Hughes, J., Richardson, P.J., Mizuguchi, K., Jackson, A.P., 2000. Beta 3: an additional auxiliary subunit of the voltage-sensitive sodium channel that modulates channel gating with distinct kinetics. Proc. Natl. Acad. Sci. U.S.A. 97, 2308–2313.

Mujtaba, M.G., Wang, S.Y., Wang, G.K., 2002. Prenylamine block of Nav1.5 channel is mediated via a receptor distinct from that of local anesthetics. Mol. Pharmacol. 62, 415–422.

Nau, C., Seaver, M., Wang, S.Y., Wang, G.K., 2000a. Block of human heart hH1 sodium channels by amitriptyline. J. Pharm. Exp. Ther. 292, 1015–1023.

Nau, C., Wang, S.Y., Strichartz, G.R., Wang, G.K., 2000b. Block of human heart hH1 sodium channels by the enantiomers of bupivacaine. Anesthesiology 93, 1022–1033.

Nuss, H.B., Kambouris, N.G., Marban, E., Tomaselli, G.F., Balser, J.R., 2000. Isoform-specific lidocaine block of sodium channels explained by differences in gating. Biophys. J. 78, 200–210.

Pugsley, M.K., Goldin, A.L., 1998. Effects of bisaramil, a novel class I antiarrhythmic agent, on heart, skeletal muscle and brain Na^+ channels. Eur. J. Pharmacol. 342, 93–104.

Tunnicliff, G., 1996. Basis of the antiseizure action of phenytoin. Gen. Pharmacol. 27, 1091–1097.

Willow, M., Gonoi, T., Catterall, W.A., 1985. Voltage clamp analysis of the inhibitory actions of diphenylhydantoin and carbamazepine on voltage-sensitive sodium-channels in neuro-blastoma cells. Mol. Pharmacol. 27, 549–558.

Yu, F.H., Westenbroek, R.E., Silos-Santiago, I., McCormick, K.A., Lawson, D., Ge, P., Ferriera, H., Lilly, J., DiStefano, P.S., Catterall, W.A., Scheuer, T., Curtis, R., 2003. Sodium channel beta 4, a new disulfide-linked auxiliary subunit with similarity to beta 2. J. Neurosci. 23, 7577–7585.